Galaxy Luminosity Function: Schechter Fxn

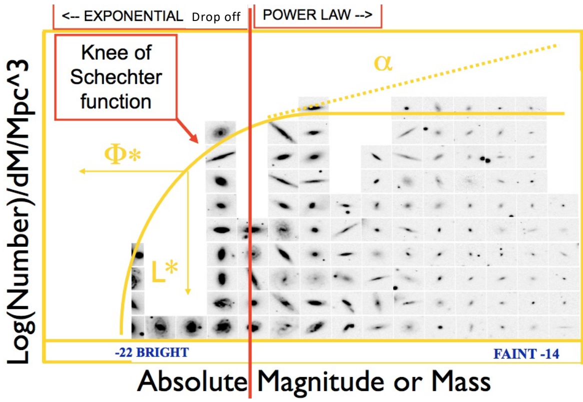

1

Schechter Fxn (in terms of Lsun)

$$\Phi(L)dL = n_*\left(\frac{L}{L_*}\right)^{\alpha} e^{-(L/L_*)}\frac{dL}{L_*}$$

$n_* = 8 \times 10^{-3}h^3\ \mathrm{Mpc}^{-3}$ $\qquad L_* = 1.4 \times 10^{10}L_\odot$ $\qquad \alpha = -0.7$

Schechter Fxn (in terms of magnitude)

$$\Phi(M)dM = (0.4ln10)\phi_* 10^{0.4(M_*-M)(\alpha+1)}e^{-10^{0.4(M_*-M)}}dM$$

$\phi_* = 1.66 \pm 0.08 \times 10^{-2}h^3\mathrm{Mpc}^{-3}$ $\qquad \alpha = -0.81 \pm 0.04$ $\qquad M^* = M^*_k = -23.19 \pm 0.04 - 5\log(h)$

$h = H_0/(100\ \mathrm{km/s/Mpc})$. Where $H_0 = 70.4\ \mathrm{km/s/Mpc}$

2

Low Luminosities…

Blanton+2005 ApJ 631

$$\Phi(M) = 0.4\ln 10\, dM\, \exp\left[-10^{-0.4(M-M_*)}\right]$$
$$\times\left[\phi_{*,1}10^{-0.4(M-M_*)(\alpha_1+1)} + \phi_{*,2}10^{-0.4(M-M_*)(\alpha_2+1)}\right]$$

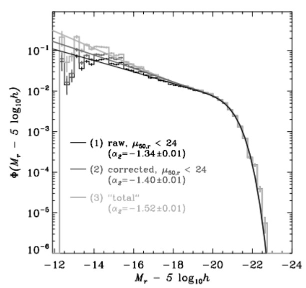

FIG. 7.—Luminosity function in the r band, calculated using the stepwise maximum likelihood method, with bins of width 0.25 mag. The black histogram indicates the minimal luminosity function, LF 1, for galaxies with $\mu_{50,r} < 24$, described in § 4.1, with no correction for surface brightness selection effects. The dark gray histogram indicates the luminosity function for galaxies with $\mu_{50,r} < 24$, corrected for surface brightness incompleteness. The light gray histogram represents an attempt to estimate how many galaxies there might be by using a simple model for the luminosity–surface brightness relationship. The values used in this plot are given in Table 2. The smooth curves are double Schechter function fits to each result, whose parameters are given in Table 3. All magnitudes here and elsewhere in the paper are K-corrected to rest-frame bandpasses and have no evolution correction applied.

3

Luminosity Function for the Stellar Disk of the Milky Way

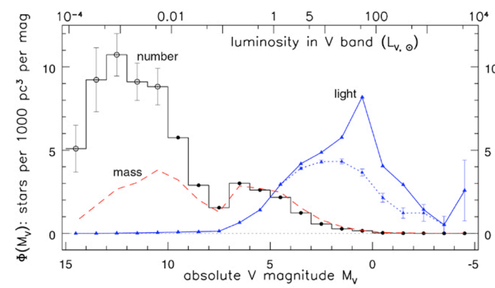

Fig 2.3 'Galaxies in the Universe' Sparke/Gallagher CUP 2007

The histogram shows the luminosity function $\Phi(M_V)$ for nearby stars. Lines with triangles show $L_V\Phi(M_V)$, light from stars in each magnitude bin; the dotted curve is for main sequence stars alone, the solid curve for the total. The dashed curve gives $\mathcal{M}\ \Phi_{MS}(M_V)$, the mass in main sequence stars. Units are $L_\odot$ or $\mathcal{M}_\odot$ per 10 pc^3; vertical bars show uncertainty.

4

$$\frac{L}{L_\odot} \approx 0.23 \left(\frac{M}{M_\odot}\right)^{2.3} \qquad (M < 0.43 M_\odot) \qquad \frac{L}{L_\odot} = \left(\frac{M}{M_\odot}\right)^{4} \qquad (0.43 M_\odot < M < 2 M_\odot) \tag{7}$$

$$\frac{L}{L_\odot} \approx 1.5 \left(\frac{M}{M_\odot}\right)^{3.5} \qquad (2 M_\odot < M < 20 M_\odot) \qquad \frac{L}{L_\odot} \approx 3200 \frac{M}{M_\odot} \qquad (M > 20 M_\odot) \tag{8}$$

Main Sequence

6

6

Initial Mass Function: $\xi(M)dM = \xi_0 (M/M_\odot)^{-\alpha} \frac{dM}{M_\odot}$

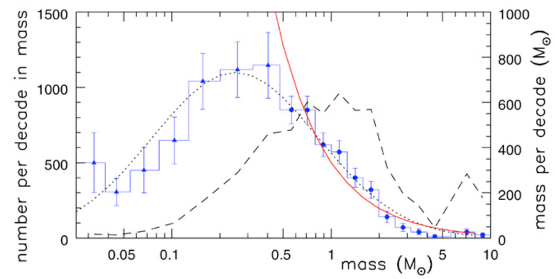

Fig 2.5 (E. Moreau) 'Galaxies in the Universe' Sparke/Gallagher CUP 2007

Masses of stars in the Pleiades cluster: The smooth red curve shows the Salpeter initial mass function, the dotted curve is a lognormal function. The dashed line shows the **mass function**: stars near 0.25 M⊙ are most numerous, but those of (1-2)M⊙ account for most of the cluster's mass.

7

7

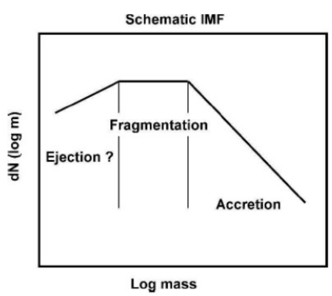

Fig. 11.— A schematic IMF showing the regions that are expected to be due to the individual processes. The peak of the IMF and the characteristic stellar mass are believed to be due to gravitational fragmentation, while lower mass stars are best understood as being due to fragmentation plus ejection or truncated accretion while higher-mass stars are understood as being due to accretion.

8

8

α- 1

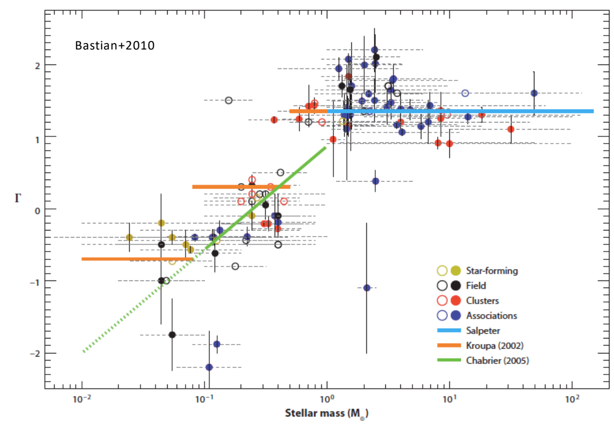

9

9

Geha+2013

Is the IMF slope at ~1 Msun actually universal?

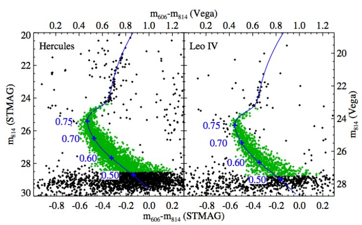

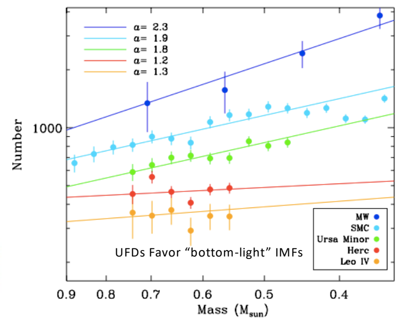

Figure 4. Stellar mass functions for the five galaxies in which the IMF has been measured via direct star counts: the Milky Way (blue; Bochanski et al. 2010), the SMC (light blue; Kalirai et al. 2013), Ursa Minor dSph (green; Wyse et al. 2002), Leo IV (yellow; this work) and Hercules (red; this work). Except for Hercules, the vertical normalization is arbitrary. For reference, the published power law slopes are shown for each dataset, normalized at 0.75 $M_\odot$. We note that a power law slope of $\alpha = 1$ is a flat line in this log–log plot. The UFD galaxies show noticeably flatter mass functions in this mass range.

10

α- 1

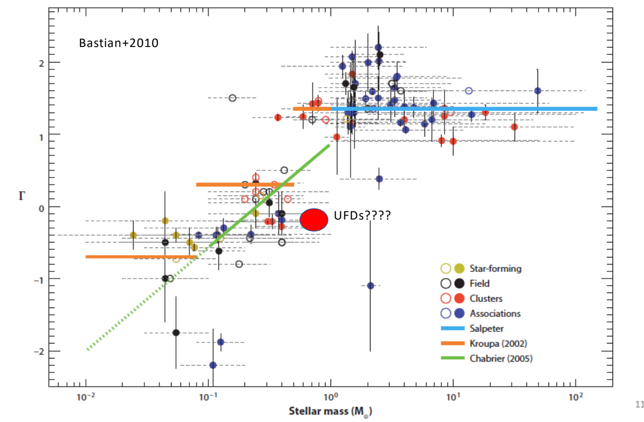

11

In the Era of JWST: ERS Proposal PI Weisz

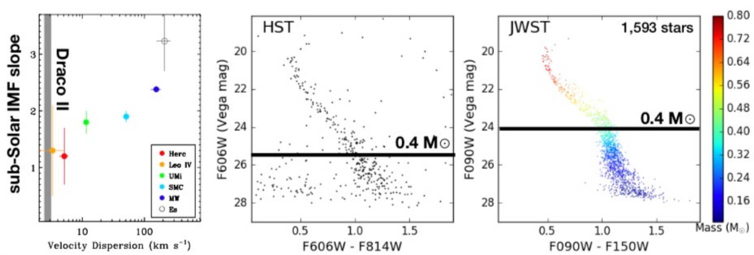

FIGURE 3: **Left–**A plot showing that galaxies with lower velocity dispersions tend to have 'bottom-light' sub-Solar IMF slopes as measured from resolved stars (Geha et al. 2013; Kalirai et al. 2013). **Middle & Right–** The *HST*-based CMD and a simulated *JWST* CMD of Draco II. The horizontal line indicates equivalent stellar masses. The sub-Solar IMF slopes of Hercules and Leo IV were measured from similarly deep *HST* data. The increased depth of our Draco II data will provide for the most secure extragalactic sub-Solar IMF measurement to date.

12